

Nested Scale-Editing for Conditional Image Synthesis

Lingzhi Zhang* Jiancong Wang* Yinshuang Xu Jie Min
Tarmily Wen James C. Gee Jianbo Shi

University of Pennsylvania

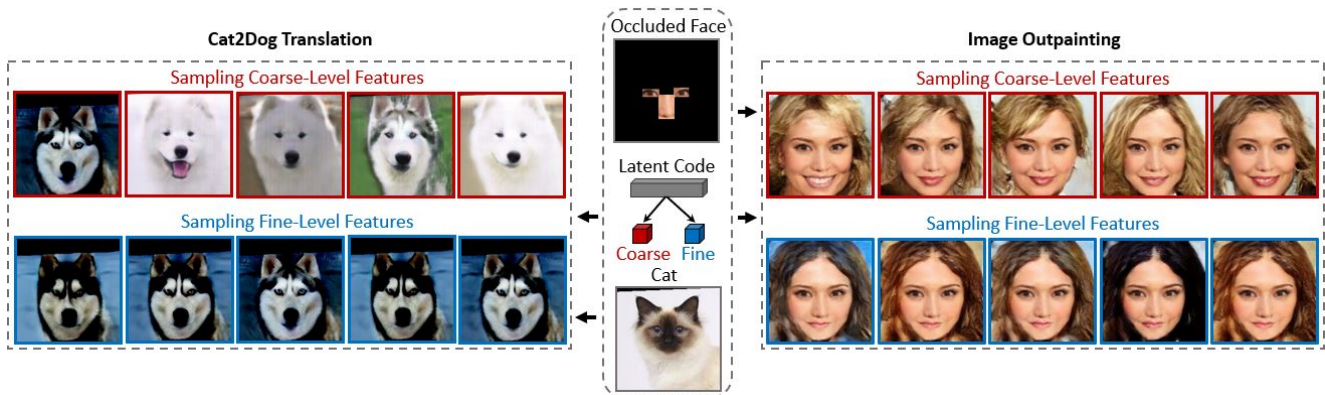


Figure 1: Our approach enables scale-specific visual editings in conditional image synthesis. We can choose to surgically manipulate coarse-level structural information or fine-level details in Cat2Dog translation and image outpainting tasks.

Abstract

We propose an image synthesis approach that provides stratified navigation in the latent code space. With a tiny amount of partial or very low-resolution image, our approach can consistently out-perform state-of-the-art counterparts in terms of generating the closest sampled image to the ground truth. We achieve this through scale-independent editing while expanding scale-specific diversity. Scale-independence is achieved with a nested scale disentanglement loss. Scale-specific diversity is created by incorporating a progressive diversification constraint. We introduce semantic persistency across the scales by sharing common latent codes. Together they provide better control of the image synthesis process. We evaluate the effectiveness of our proposed approach through various tasks, including image outpainting, image superresolution, and cross-domain image translation.

1. Introduction

Imagine that we want to identify a person based on the appearance of their eyes and nose, or a lower resolution image, as shown in figure 1. One solution may be to outpaint the entire face, conditioned on the partial information available.

*equal contribution.

We want to be as imaginative and as detailed as possible to give us a greater chance of success in finding the right person. These tasks are multimodal in nature, i.e., a single input corresponds to many plausible outputs.

Conditional image synthesis approaches aim to solve this problem by sampling stochastic latent codes to generate images in a GAN setting. However, these image synthesis methods of sampling operate as uncontrollable black boxes. During inference, we can only hope that a sampled random variable generates the ideal image we desire; otherwise, we need to keep sampling.

We propose a steerable conditional image synthesis approach. Inspired by the steerable filtering in the wavelet process [50], we wish to ‘steer’ the image synthesis across the spatial scales consistently. While in steerable filtering we are concerned with angular edge orientation, in our domain, we focus on object semantics. Specifically, we aim to create visual information from a coarse-level structure to fine-level texture. The key objectives are 1) **scale-independence**: we learn disentangled representations that model scale-specific visual details, and 2) **diversity/mode covering**: we ensure that the decoder covers diverse variations presented on ground truth images.

To implement the scale-independent objective, we take inspiration from the Laplacian image pyramid decomposi-

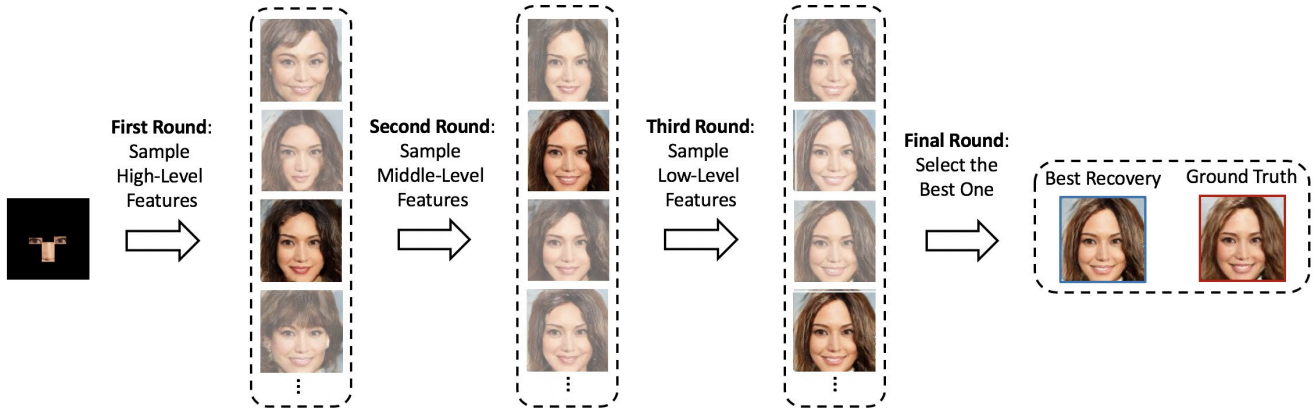


Figure 2: Demonstration of an application scenario in which a user interactively recovers a facial identity by sampling scale-specific visual details using our proposed approach. Image you look at this occluded face, you might have a rough mental picture of someone. We can edit the image at multi-scale to recover the identity.

tion: our algorithm essentially learns to generate progressively more refined image along spatial scales, with each level of refinement independent of each other. To implement the diversity objective, we extend a successful diversity constraint [37] to multi-scale and ensure scale-specific diversity.

Unlike current multi-scale noise injection methods [7, 25], our multi-scale injected noises share *same* latent variable during training. This introduces semantic persistency, meaning the decoder expects latent variables on different scales to have similar semantic meaning. Semantic-persistence can play a major role in search efficiency, since it enables stratified navigation in the latent code space. Fig.2 illustrates the stratified navigation process for face super-resolution. We first coarsely sample a widespread set of latent random variables to find an image roughly matching the ground truth. Because of our scale-independent representation, we can efficiently edit the image by adjusting any of the latent variable at a specific scale and edit the image information at the corresponding scale. Therefore we can generate a refined image by adjusting the existing latent variable at next scale and repeat, until final scale is reached. This is the ideal steering behavior we seek.

In summary, we highlight our contributions as follows:

- We are the first to propose a multi-scale feature disentanglement loss and a progressive diversification regularization to achieve scale-specific control for conditional image synthesis.
- To the best of our knowledge, our work is the first to utilize diverse conditional image generation for identity recovery. We developed three evaluation metrics for identity recovery in diverse conditional synthesis scenarios.
- We evaluate our aforementioned development on tasks of image outpainting, image superresolution, and mul-

timodal image translation. Our methods achieves competitive image quality and diversity compared to state-of-the-art counterparts, while consistently outperforming them in terms of identity recovery.

2. Related Work

2.1. Multimodal Conditional Generation

Deep generative models have been widely used in many conditional image synthesis tasks, such as super-resolution [9, 28, 57, 63–65], inpainting missing regions [21, 36, 44, 45, 59, 61, 62, 68], style transfer [15, 18, 22, 35, 40], image blending [41, 51, 58, 69], and text-to-image [23, 33, 47]. The majority of these tasks are in nature multimodal, where single input condition may correspond to multiple plausible outputs. BicycleGAN [71] first proposed to model this one-to-many distribution by explicitly encoding the target domain into a compact Gaussian latent distribution from which the generator samples. During inference, the generator maps a random variable drawn from the latent distribution, combined with the given input, to the output. StackedGAN and its variant StackedGAN++ [66, 67] proposed to use a hierarchical generator which incorporates conditional code on multiple scales and were able to generate high quality synthetic images. DRIT [32] and MUNIT [20] proposed to disentangle the features into domain-invariant content codes and domain-specific style codes for unpaired image-to-image translations. During inference, the sampled style codes combined with the content code can be transformed into many plausible outputs.

Although the above approaches can generate multimodal outputs given a conditional input, there is no explicit constraint to prevent the generator from mapping the various sampled random variables to similar outputs, which is known as mode collapse. Two concurrent works aim to al-

leviate this issue by proposing diversity regularization techniques for generative training. Mode Seeking GAN (MSGAN) [42] proposes to maximize the ratio of two sampled images over the corresponding latent variables. Normalized Diversification (NDiv) [37] proposes to enforce the generator to preserve the normalized pairwise distance between the sparse samples from a latent distribution to the corresponding high-dimensional output space.

In addition to image synthesis, other applications with multimodal predictions include but are not limited to predicting uncertain motion flows in the future [14, 54, 60], hallucinating diverse body pose affordance in 2D [55] and 3D [34] scenes.

Different from previous work, our focus is to achieve scale-specific control for image synthesis and progressively inject stochasticity into different scales of the synthesized image. Therefore, our proposed techniques can be readily added into these orthogonal previous approaches. We demonstrate that our techniques work with face outpainting, face superresolution, and multimodal animal translation with modified MUNIT [20].

2.2. Feature Disentanglement

Recently there is increasing interest in disentanglement of distinct image characteristics for image synthesis. [26, 30, 56] attempt to decouple image style and content, while [12, 13, 39] target object shape and appearance. These approaches explicitly incorporate two codes that denote the two characteristics, respectively, into the generative model and introduce a guided loss or incorporate the invariance constraint to orthogonalize the two codes, while our method disentangles the scale-specific variations from global structural feature to local texture feature through hierarchical input of latent variables into the generative model.

Besides the disentanglement of two specific characteristics, several prior efforts [4, 5, 8, 10, 17] have explored partially or fully interpretable representations of independent factors for generative modeling. Some current work learn representations of the specific attribute by supervised learning [2, 46] with a conditioning discriminator. Our method focuses on multi-scale disentanglement through unsupervised learning, which is distinct from the concept of disentangling specific semantic factors.

[24] has first proposed synthesize images from low-resolution scale to higher-resolution scale in a progressive manner. Similarly, other closely related work is [7] and [25]. [7] pioneered the use of the hierarchical generator with latent codes injected at each level for multi-scale control of image synthesis and further advanced in [25]. Both [7] and [25], however, only target unconditional image synthesis and do not explicitly enforce diversity of outputs. Our work extends to conditional synthesis and incorporates explicit diversity constraints.

Since the purpose and definition of disentanglement in our method are different from previous work, the existing metrics for evaluating disentanglement [4, 11, 17, 25, 27] are not appropriate for measuring feature disentanglement for our method. We therefore develop a new means to quantify the hierarchical disentanglement for our approach.

3. Methods

Multimodal conditional image synthesis combines a given input conditional code with sampled latent codes drawn from a compact latent space (usually a standard normal or uniform distribution) and decodes the combination into an output image. Unlike previous efforts [20, 37, 42, 71], we propose a cascading disentangled decoder inspired by Laplacian image pyramid [1]. With a central multi-scale backbone, it generates output images at every feature spatial scale through a single convolutional layer. We enforce the generated images at every scale to be average-pooled back into a lower-resolution generated image. By doing so, we distill features at each spatial scale to only focus on image details — similar to a Laplacian image — at the corresponding spatial resolution. With these scale-independent features, we can inject random variables into each scale of the image features to model the scale-specific stochasticity of image details.

3.1. Multiscale Disentanglement

To enable scale-specific editing of visual contents, we need a model that has a disentangled latent code representation. This implies that visual content on specific scales can be modified by changing corresponding latent codes, while visual contents on other scales remain unaffected.

In a decoder network that receives only a single latent code at the coarsest scale, the single latent code controls image generation at all scales and hence changing the code will affect all scales. This motivates the multi-latent code design: injecting latent codes on all spatial scales and allowing each individual latent code to control the image on corresponding scales. Let Z_0 denote the random base latent code, and $Z_1 = A_1(Z_0)$, $Z_2 = A_2(Z_0)$, \dots , $Z_k = A_k(Z_0)$, and the latent variable at each scale level $i \in \{1 \dots k\}$, where A_i is an affine mapping matrix. Intuitively, the latent code at coarse scale may mostly affect global structure while latent code at fine scale is more likely to alter local texture at its respective scale. Such behavior can be seen in [7] and [25].

However, this design does not guarantee that visual information represented by the latent code at different scales are disentangled. For example, latent code at coarse scale might control texture and color that are also affected by latent code at fine scale. With such a decoder, it is still difficult to edit the scale-specific visual information while keeping information on other scales unchanged.

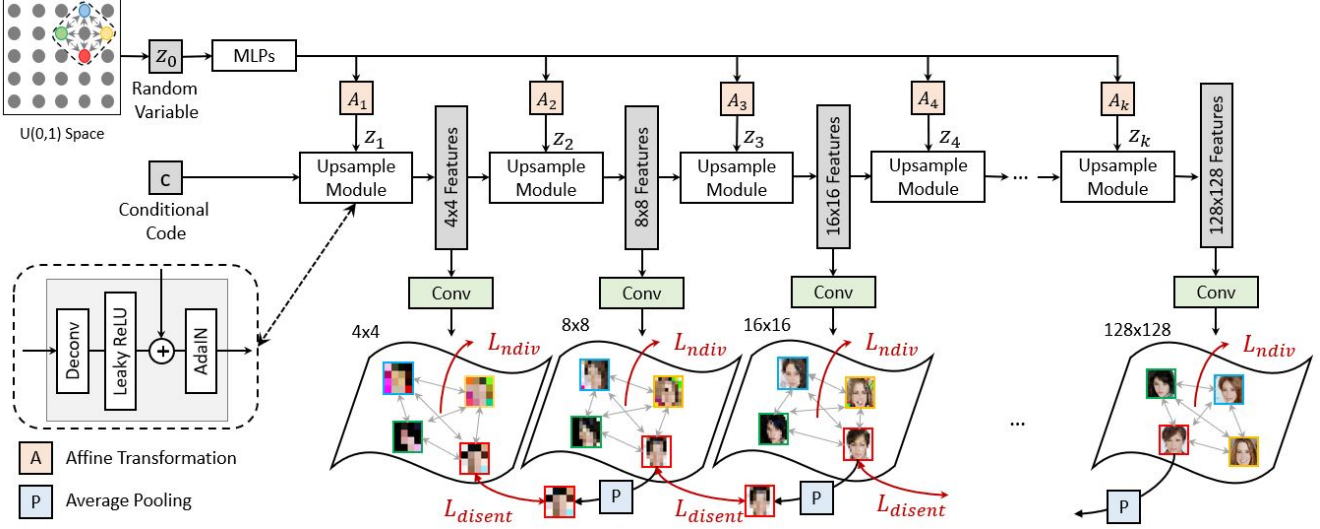


Figure 3: Our decoder network takes a conditional code and a single random variable as inputs. A single latent variable is injected into multi-scale feature representations through the first several shared layers of MLPs. Then that output is injected into different affine transformation layers with Adaptive Instance Normalization (AdaIN) [19]. At every spatial scale, a single convolutional layer is used to decode a real image at each corresponding resolution. Our proposed disentanglement loss enforces the generated images at every scale to be averaged-pooled back into a lower-resolution generated image. At each iteration, we sample four latent variables and generate four images at each spatial scale, where we also enforce the pairwise distance between sampled images and latent variables to encourage diverse synthesized outputs.

Therefore, we propose a simple but effective approach to disentangle features at each layer of the decoder to only control the visual information at the corresponding spatial scale. At each layer in the decoder, we add a single convolutional layer to synthesize an image at the corresponding spatial resolution. Then, we enforce that each synthesized image, when downsampled, matches the synthesized image at the previous spatial scale. We call this constraint a multi-scale disentanglement loss L_{disent} . Specifically, we use average pooling to downsample the synthesized image and pixel-wise Euclidean distance to constraint the downsampling consistency. Our intuition is that, by doing so, the features at each layer are not allowed to change any visual information at the previous or deeper layers. In this way, we distill each level of features to only edit the visual information at its corresponding spatial scale.

Formally, we denote S as the downsampling operation on image x , specifically, average 2×2 pooling with stride of 2. The loss function of progressive downsampling consistency is defined as follows,

$$\mathcal{L}_{disent} = \sum_{i=1}^{n-1} d(S(G_{i+1}(c, z)), G_i(c, z)), \quad (1)$$

where n is the number of resolution scales, c is the conditional code, z is random variable, and G_i is the generator, whose subscript refers to the network layers that

are responsible for synthesizing images at each scale. For $G_i (2 \leq i \leq n)$, they have iterative format:

$$G_i(c, z) = U[G_{i-1}(c, z), A_i(z)] \quad (2)$$

and,

$$G_1(c, z) = U[c, A_1(z)]. \quad (3)$$

where U denotes the Upsampling Module.

At each spatial scale, we also applied conditional GAN to synthesize photo-realistic images, where the loss functions are as follows,

$$\mathcal{L}_{GAN} = E_{\mathbf{x} \sim p_{data}(\mathbf{x})} \left[\sum_{i=1}^n \log(D_i(S^{n-i}(\mathbf{x})|c)) \right] + E_{\mathbf{z} \sim p(\mathbf{z})} \left[\sum_{i=1}^n \log(1 - D_i(G_i(\mathbf{z}, c))) \right]. \quad (4)$$

The similar multi-scale adversarial loss has been applied in SinGAN [49] as well.

3.2. Progressive Diversification

To avoid mode collapse and increase diversity of the synthesized images, we leverage the normalized diversification [37], which forces the normalized pairwise distance of generative outputs to be at least as large as that of the corresponding latent variables.

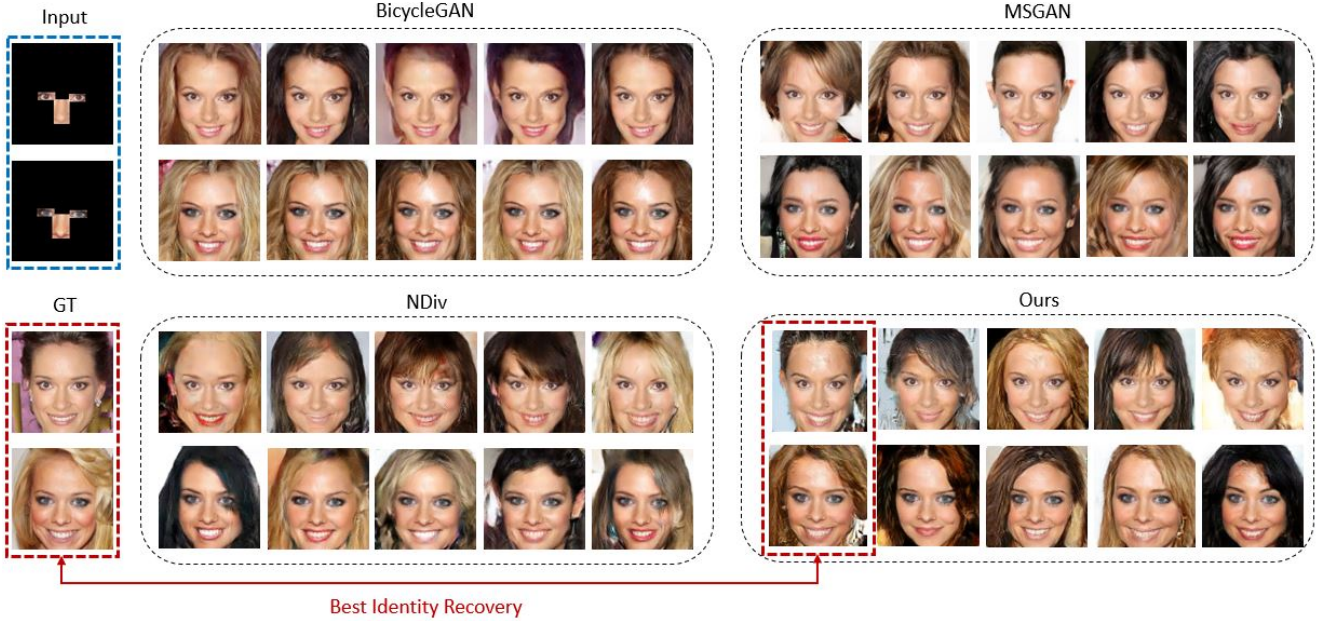


Figure 4: Qualitative comparison for multimodal image outpainting.

Method	Quality ↓	Diversity ↑	Identity		
			Shortest Distance ↓	Recovery Count(%) ↑	Landmark Alignment ↓
BicycleGAN	64.133	0.093	0.233	15.34	5.914
MSGAN	56.998	0.232	0.237	28.93	4.754
Ndiv	68.855	0.319	0.256	20.95	5.126
Ours	55.854	0.333	0.228	34.78	4.540

Table 1: Quantitative Comparison with state-of-the-art approaches in multimodal image outpainting task.

Here we introduce normalized diversification in a progressive manner, that is, we add normalized diversification loss at each layer of the hierarchical decoder. In comparison, previous work [37, 42, 43] applied the diversity penalty only at the final scale output of the model, which enforces in a brute force way the final output diversity but does not prevent individual levels of the model from mode collapse (for a 3-layer model where latent code z is injected at each level, previous efforts only enforce that the final output varies by z , but allow individual layers to collapse. For example, the first layer of the model utilizes the z while second and third layer ignore z entirely).

Mode collapses at individual levels prevent us from exactly controlling the diversity on a specific level of structure or texture for synthesized data. Thus, we propose progressive diversification, effectively unfolding manifold topology for different scales. In this way, we achieve not only independent multi-scale control during the generative process but also guarantee latent that the code z introduces variation on every scale, likely from structure to texture.

The inserted progressive normalized diversification can

be formulated as loss function 5.

$$\mathcal{L}_{Ndiv} = \sum_{k=1}^n \frac{1}{N^2 - N} \sum_{i=1}^N \sum_{j=1}^N \max(\alpha D_{ij}^z - D_{ij}^{G_k(z,c)}), \quad (5)$$

where N is the number of samples to calculate the normalized pairwise distance matrix and $D_{ij}^z, D_{ij}^{G_k(z|y)}$ are defined as elements in normalized pairwise distance matrix $D^z, D^{G_k(z|y)} \in \mathbb{R}^{N \times N}$ of $z_{i=1}^N \sim p(z)$:

$$D_{ij}^z = \frac{d(z_i - z_j)}{\sum_j d(z_i - z_j)} \quad (6)$$

$$D_{ij}^{G_k(z,c)} = \frac{d(G_k(z,c)_i - G_k(z,c)_j)}{\sum_j d(G_k(z,c)_i - G_k(z,c)_j)}.$$

Here, d the latent variable is the Euclidean distance, and for generative outputs is the pixel-wise Euclidean distance.

4. Experiments

The proposed approaches were evaluated through their performance on various tasks, including image outpainting,

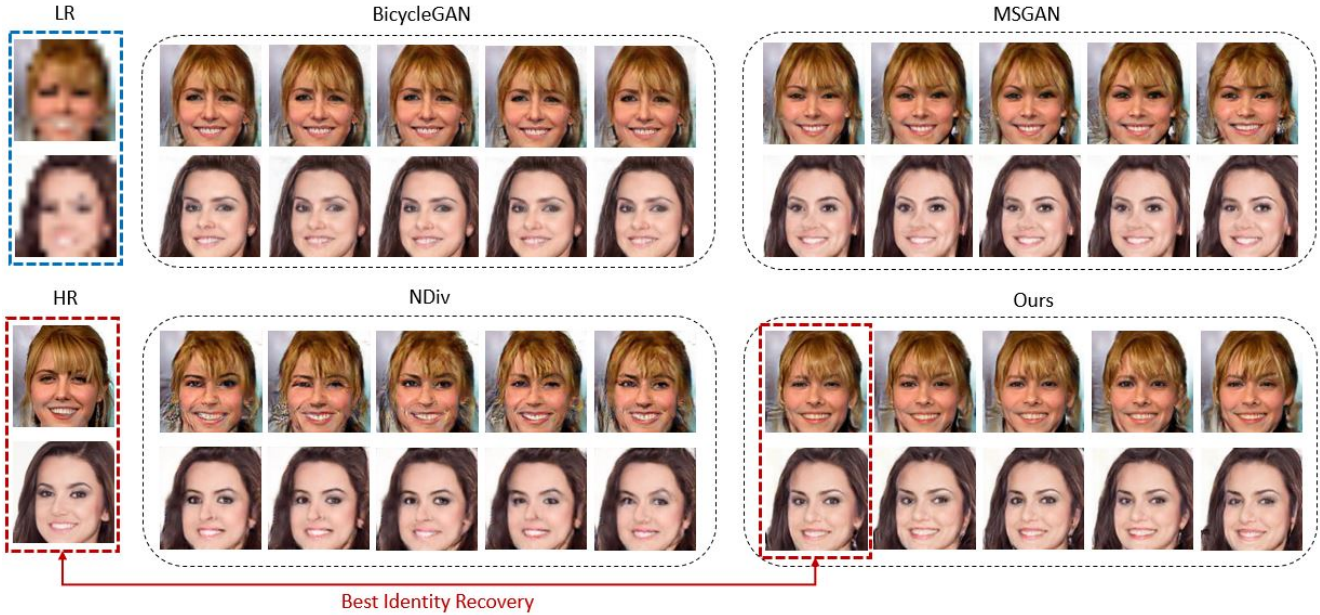


Figure 5: Qualitative comparison for multimodal image superresolution

Method	Quality ↓	Diversity ↑	Identity		
			Shortest Distance ↓	Recovery Count(%) ↑	Landmark Alignment ↓
BicycleGAN	40.837	0.019	0.129	26.49	7.062
MSGAN	49.647	0.0438	0.131	29.48	5.907
Ndiv	81.4213	0.0758	0.143	5.60	5.938
Ours	46.346	0.0677	0.125	38.43	4.261

Table 2: Quantitative Comparison with state-of-the-art approaches in multimodal image superresolution task.

image superresolution, and dog2cat/cat2dog translation. In addition to conventional quality and diversity assessment, we propose to evaluate the extent to which diverse sampling can improve identity recovery, especially in the context of facial recognition. We believe that this is a first attempt that aims to apply diverse synthesis for better recognition. Our premise is that given a conditional code containing only partial information of the ground truth image, a decoder capable of generating diverse output can produce at least one or more results that is close to or recovers the ground truth image, as long as sufficient latent code is sampled. This property would be useful in many difficult recognition situations, such as identifying criminals in largely occluded or very low-resolution images. Diverse sampling would provide a set of candidates, which can then be narrowed down further by human reviewers. We describe next three newly proposed evaluation metrics in this work for identity recovery.

4.1. Evaluation Metrics

To perform evaluation of our approach, we use the following metrics.

FID. We use FID [16] to evaluate the quality of generated

data. This metric applies the Inception Network [52] to extract features from real and synthesized data, and then calculates the Frechet distance between the two distributions of collected real and synthesized features, respectively. A lower FID score indicates less discrepancy between real and synthesized data and hence higher quality.

LPIPS. We apply LPIPS [70] to quantify the diversity, which calculates the pairwise average feature distance across the whole generated dataset. We use AlexNet [31] pretrained on ImageNet [6] to extract features. Larger values of the pairwise LPIPS score indicate increased image diversity.

Identity Recovery. To quantify how well diverse sampling recovers the true facial identity, we propose to evaluate the distance between the most similar sampled output and the ground truth image. First, we compute the shortest embedding distance between a set of sampled outputs and the ground truth, where the embedding distance is given by LPIPS. We average this shortest embedding distance across all training examples, which we denote as **Shortest Distance** in Table (1) and (2). We also count the chance that each method generates the most similar outputs under evaluation of this embedding distance, and denote this as **Re-**

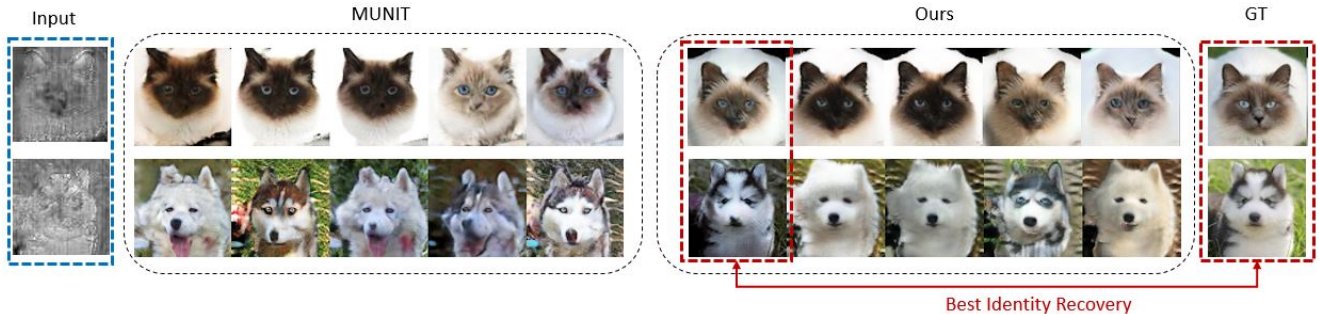


Figure 6: Qualitative comparison against the state-of-the-art in multi-modal translation for cat/dog identity recovery. The input (left column) indicates a MUNIT content code. Only one channel of the content code is shown for easier .

Method	Quality ↓	Diversity ↑	Identity	
			Shortest Distance ↓	Recovery Count(%) ↑
MUNIT [20]	15.74	0.533	0.445	15.0
Ours	21.22	0.547	0.393	85.0

Table 3: Quantitative comparison with state-of-the-art approaches on the cross-modal image-to-image translation task.

covery Count. We also evaluate the identity recovery of face images using facial landmarks, which are obtained using a pretrained facial landmark detector [3]. Specifically, the similarity between a sampled output and the ground truth is given by the mean squared error distance between the corresponding 68 facial landmark locations for the sampled and ground-truth images. We refer to this evaluation as **Landmark Alignment**.

4.2. Image Outpainting

We first present experimental results in an image outpainting task, where the goal is to fill in large areas of missing pixels in a highly occluded image, which may have many different solutions for a given input. In terms of model implementations, we only need to add our proposed multi-scale disentanglement and diversification into a standard conditional encoder-decoder. The experiment is conducted over the CelebA dataset [38] with cropped 128x128 images.

We compare our model with the current state-of-the-art multimodal conditional synthesis approaches, including BicycleGAN [71], MSGAN [42], and NDiv [37]. The experimental results show that our model can generate the best results in terms of image quality, diversity as well as identity, as shown in Table.1. In our qualitative comparison figure.4, we show that one of the sampled image could best recover the ground truth facial identity. We think that this is because our model can sample not only very diverse but also realistic images.

4.3. Image Super-Resolution

Another multimodal conditional synthesis we run on face data is super-resolution. While most of other super-resolution approaches model this task as a deterministic

image-to-image process, we consider super-resolution from a very low resolution image as a one-to-many process because of its uncertainty in nature. For example, the 16x16 low resolution in Figure.5 can be very difficult to identified. Even for human, it is very difficult to tell what is the ground true high-resolution image is. Or, every human would probably have a different answer. In this task, we use bilinearly downsampled 16x16 image as low-resolution input and 128x128 image as high-resolution output in CelebA dataset [38].

Our implementation of superresolution model is similar to image outpainting, but we start to decode image at scale of 16x16, which is the same as input resolution. The disentanglement and diversification is added at every other higher resolution scale. As seen from Table. (2), even though our approach does not reach the best quality or diversity, but it achieves the best identity score. We think that the simply measuring quality or diversity separately is not sufficient. BicycleGAN has the best quality but lack diversity, so it is difficult to hit the ground truth image. NDiv has the largest diversity but lacks quality, and thus it is also very difficult to recover the realistic ground truth image. In contrast, our model can produce reasonably large diversity and good quality, and thus has the highest chance to recover the ground truth image. Our implementation of super-resolution model is similar to image outpainting, but we start to decode image at scale of 16x16, which is the same as input resolution. The disentanglement and diversification is added at every other higher resolution scale. As seen from Table. (2), even though our approach does not reach the best quality or diversity, but it achieves the best identity score. We think that the simply measuring quality or diversity separately is not sufficient. BicycleGAN [71] has

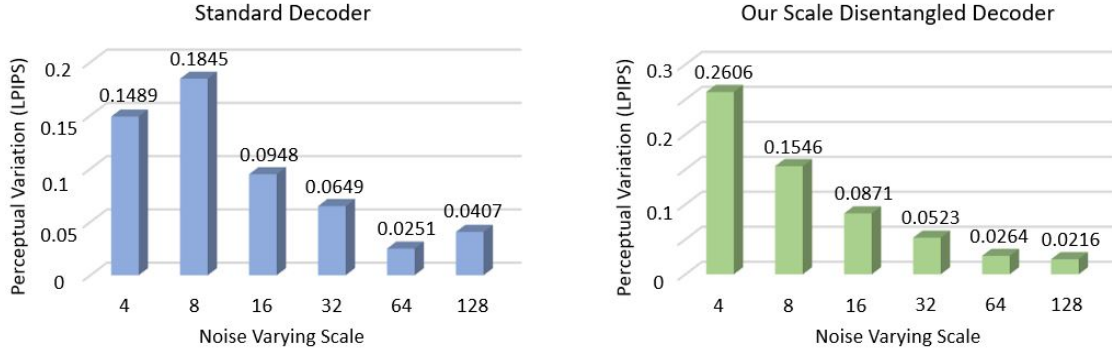


Figure 7: This figure demonstrates how much the generated image would change by varying noise injection at a specific resolution scale. This is implemented by sampling a reference code, and only varying random variable at one scale at a time and fixing the random variables at the other scales constant.

the best quality but lack diversity, so it is difficult to hit the ground truth image. NDiv [37] has the largest diversity but lacks quality, and thus it is also very difficult to recover the realistic ground truth image. In contrast, our model can produce reasonably large diversity and good quality, and thus has the highest chance to recover the ground truth image.

4.4. Dog to Cat Image Translation

We conduct an unpaired cross-modal image translation using the MUNIT backbone [20] on the cat and dog dataset from [32]. This dataset contains 1264 training/100 testing dog and 771 training/100 testing cat images. We modify the MUNIT backbone for multi latent codes injection and implemented the disentanglement loss and progressive diversification loss as mentioned in section 3.1 and 3.2. Detailed network architecture before and after modification can be found in the supplemental material. We compare FID and LPIPS of our model against the original MUNIT model trained on the cat and dog dataset and report the performance in Table.3. For identity recovery evaluation, we pass the ground truth image through the content encoder from the MUNIT framework and derive a content code, which is recombined with sampled latent codes and decoded into images. Quantitatively, we evaluate identity recovery using the LPIPS metric from 4.1. Qualitative results of identity recovery is demonstrated in Fig.6.

4.5. Multi-scale Disentanglement Evaluation

To quantify the multiscale disentanglement, we evaluate perceptual variations on output images against different noise varying scales. In specific, for scale k in our n scale decoder, a given fixed input condition code c , we sample a center latent code z . We fixed the input latent codes on every scale to be z except for for scale k , where we sample 10 latent codes centered around z and generate 10 different output images. Pairwise perceptual distances (using LPIPS) among these 10 images are calculated. We calculate

the pairwise perceptual distance for scale k across 1000 different input condition codes and averaged them. We plotted the averaged perceptual distance against the scale on Fig.8. For a general decoder (left) without the the disentanglement constraint, the perceptual variation were not monotonically decreasing along the scale. Our scale disentangled decoder (right) on the other hand achieves multiscale disentanglement: latent codes at finer scales monotonically introduce less variation to the image, therefore editing latent code at finer level has little effect on visual information on coarse scale.

5. Conclusion

We develop a conditional image synthesis network that enables scale-specific and diverse control of image content. We instantiate our design with a cascading decoder network. We couple it with multi-scale feature disentanglement constraints and a progressive diversification regularization. In addition, we gain semantic persistency in the decoder by sharing latent code across scales during training. This allows for stratified navigation and search within latent code space, and motivate the task of identity recovery. We propose three evaluation metrics for identity recovery within conditional image synthesis scenarios. On tasks of image outpainting, image superresolution, and multimodel image translation, our method consistently outperforms state-of-the-art counterparts in terms of identity recovery, while having competitive image quality and diversity. Hence we believe our method may potentially be useful in extreme image recognition situations, such as recognizing criminals in largely occluded or very low-resolution images, and finding lost pets from low quality surveillance images.

Acknowledgement

We gratefully appreciate the support from Honda Research Institute Curious Minded Machine Program. We also

gratefully acknowledge a GPU donation from NVIDIA.

References

- [1] Edward H Adelson, Charles H Anderson, James R Bergen, Peter J Burt, and Joan M Ogden. Pyramid methods in image processing. *RCA engineer*, 29(6):33–41, 1984. [4323](#)
- [2] Grigory Antipov, Moez Baccouche, and Jean-Luc Dugelay. Face aging with conditional generative adversarial networks. In *2017 IEEE International Conference on Image Processing (ICIP)*, pages 2089–2093. IEEE, 2017. [4323](#)
- [3] Adrian Bulat and Georgios Tzimiropoulos. Super-fan: Integrated facial landmark localization and super-resolution of real-world low resolution faces in arbitrary poses with gans. In *Proceedings of the IEEE Conference on Computer Vision and Pattern Recognition*, pages 109–117, 2018. [4327](#)
- [4] Tian Qi Chen, Xuechen Li, Roger B Grosse, and David K Duvenaud. Isolating sources of disentanglement in variational autoencoders. In *Advances in Neural Information Processing Systems*, pages 2610–2620, 2018. [4323](#)
- [5] Xi Chen, Yan Duan, Rein Houthoofd, John Schulman, Ilya Sutskever, and Pieter Abbeel. Infogan: Interpretable representation learning by information maximizing generative adversarial nets. In *Advances in neural information processing systems*, pages 2172–2180, 2016. [4323](#)
- [6] J. Deng, W. Dong, R. Socher, L.-J. Li, K. Li, and L. Fei-Fei. ImageNet: A Large-Scale Hierarchical Image Database. In *CVPR09*, 2009. [4326](#)
- [7] Emily L Denton, Soumith Chintala, Rob Fergus, et al. Deep generative image models using a laplacian pyramid of adversarial networks. In *Advances in neural information processing systems*, pages 1486–1494, 2015. [4322](#), [4323](#)
- [8] Jeff Donahue, Philipp Krähenbühl, and Trevor Darrell. Adversarial feature learning. *arXiv preprint arXiv:1605.09782*, 2016. [4323](#)
- [9] Chao Dong, Chen Change Loy, Kaiming He, and Xiaoou Tang. Image super-resolution using deep convolutional networks. *IEEE transactions on pattern analysis and machine intelligence*, 38(2):295–307, 2016. [4322](#)
- [10] Vincent Dumoulin, Ishmael Belghazi, Ben Poole, Olivier Mastropietro, Alex Lamb, Martin Arjovsky, and Aaron Courville. Adversarially learned inference. *arXiv preprint arXiv:1606.00704*, 2016. [4323](#)
- [11] Cian Eastwood and Christopher KI Williams. A framework for the quantitative evaluation of disentangled representations. 2018. [4323](#)
- [12] Patrick Esser, Johannes Haux, and Bjorn Ommer. Unsupervised robust disentangling of latent characteristics for image synthesis. In *Proceedings of the IEEE International Conference on Computer Vision*, pages 2699–2709, 2019. [4323](#)
- [13] Patrick Esser, Ekaterina Sutter, and Björn Ommer. A variational u-net for conditional appearance and shape generation. In *Proceedings of the IEEE Conference on Computer Vision and Pattern Recognition*, pages 8857–8866, 2018. [4323](#)
- [14] Ruohan Gao, Bo Xiong, and Kristen Grauman. Im2flow: Motion hallucination from static images for action recognition. In *Proceedings of the IEEE Conference on Computer Vision and Pattern Recognition*, pages 5937–5947, 2018. [4323](#)
- [15] Leon A Gatys, Alexander S Ecker, and Matthias Bethge. Image style transfer using convolutional neural networks. In *Proceedings of the IEEE conference on computer vision and pattern recognition*, pages 2414–2423, 2016. [4322](#)
- [16] Martin Heusel, Hubert Ramsauer, Thomas Unterthiner, Bernhard Nessler, and Sepp Hochreiter. Gans trained by a two time-scale update rule converge to a local nash equilibrium. In *Advances in Neural Information Processing Systems*, pages 6626–6637, 2017. [4326](#)
- [17] Irina Higgins, Loic Matthey, Arka Pal, Christopher Burgess, Xavier Glorot, Matthew Botvinick, Shakir Mohamed, and Alexander Lerchner. beta-vae: Learning basic visual concepts with a constrained variational framework. *ICLR*, 2(5):6, 2017. [4323](#)
- [18] Xun Huang and Serge Belongie. Arbitrary style transfer in real-time with adaptive instance normalization. In *Proceedings of the IEEE International Conference on Computer Vision*, pages 1501–1510, 2017. [4322](#)
- [19] Xun Huang and Serge Belongie. Arbitrary style transfer in real-time with adaptive instance normalization. In *Proceedings of the IEEE International Conference on Computer Vision*, pages 1501–1510, 2017. [4324](#), [4332](#)
- [20] Xun Huang, Ming-Yu Liu, Serge Belongie, and Jan Kautz. Multimodal unsupervised image-to-image translation. In *Proceedings of the European Conference on Computer Vision (ECCV)*, pages 172–189, 2018. [4322](#), [4323](#), [4327](#), [4328](#), [4332](#), [4334](#)
- [21] Satoshi Iizuka, Edgar Simo-Serra, and Hiroshi Ishikawa. Globally and locally consistent image completion. *ACM Transactions on Graphics (ToG)*, 36(4):107, 2017. [4322](#)
- [22] Justin Johnson, Alexandre Alahi, and Li Fei-Fei. Perceptual losses for real-time style transfer and super-resolution. In *European Conference on Computer Vision*, pages 694–711. Springer, 2016. [4322](#)
- [23] Justin Johnson, Agrim Gupta, and Li Fei-Fei. Image generation from scene graphs. In *Proceedings of the IEEE Conference on Computer Vision and Pattern Recognition*, pages 1219–1228, 2018. [4322](#)
- [24] Tero Karras, Timo Aila, Samuli Laine, and Jaakko Lehtinen. Progressive growing of gans for improved quality, stability, and variation. *arXiv preprint arXiv:1710.10196*, 2017. [4323](#)
- [25] Tero Karras, Samuli Laine, and Timo Aila. A style-based generator architecture for generative adversarial networks. In *Proceedings of the IEEE Conference on Computer Vision and Pattern Recognition*, pages 4401–4410, 2019. [4322](#), [4323](#)
- [26] Hadi Kazemi, Seyed Mehdi Iranmanesh, and Nasser Nasrabadi. Style and content disentanglement in generative adversarial networks. In *2019 IEEE Winter Conference on Applications of Computer Vision (WACV)*, pages 848–856. IEEE, 2019. [4323](#)
- [27] Hyunjik Kim and Andriy Mnih. Disentangling by factorising. *arXiv preprint arXiv:1802.05983*, 2018. [4323](#)
- [28] Jiwon Kim, Jung Kwon Lee, and Kyoung Mu Lee. Accurate image super-resolution using very deep convolutional networks. In *Proceedings of the IEEE conference on computer*

- vision and pattern recognition*, pages 1646–1654, 2016. [4322](#)
- [29] Diederik P Kingma and Jimmy Ba. Adam: A method for stochastic optimization. *arXiv preprint arXiv:1412.6980*, 2014. [4332](#)
- [30] Dmytro Kotovenko, Artsiom Sanakoyeu, Sabine Lang, and Bjorn Ommer. Content and style disentanglement for artistic style transfer. In *Proceedings of the IEEE International Conference on Computer Vision*, pages 4422–4431, 2019. [4323](#)
- [31] Alex Krizhevsky, Ilya Sutskever, and Geoffrey E Hinton. Imagenet classification with deep convolutional neural networks. In *Advances in neural information processing systems*, pages 1097–1105, 2012. [4326](#)
- [32] Hsin-Ying Lee, Hung-Yu Tseng, Jia-Bin Huang, Maneesh Singh, and Ming-Hsuan Yang. Diverse image-to-image translation via disentangled representations. In *Proceedings of the European Conference on Computer Vision (ECCV)*, pages 35–51, 2018. [4322](#), [4328](#)
- [33] Wenbo Li, Pengchuan Zhang, Lei Zhang, Qiuyuan Huang, Xiaodong He, Siwei Lyu, and Jianfeng Gao. Object-driven text-to-image synthesis via adversarial training. In *Proceedings of the IEEE Conference on Computer Vision and Pattern Recognition*, pages 12174–12182, 2019. [4322](#)
- [34] Xueting Li, Sifei Liu, Kihwan Kim, Xiaolong Wang, Ming-Hsuan Yang, and Jan Kautz. Putting humans in a scene: Learning affordance in 3d indoor environments. In *Proceedings of the IEEE Conference on Computer Vision and Pattern Recognition*, pages 12368–12376, 2019. [4323](#)
- [35] Yijun Li, Chen Fang, Jimei Yang, Zhaowen Wang, Xin Lu, and Ming-Hsuan Yang. Universal style transfer via feature transforms. In *Advances in neural information processing systems*, pages 386–396, 2017. [4322](#)
- [36] Guilin Liu, Fitsum A Reda, Kevin J Shih, Ting-Chun Wang, Andrew Tao, and Bryan Catanzaro. Image inpainting for irregular holes using partial convolutions. In *Proceedings of the European Conference on Computer Vision (ECCV)*, pages 85–100, 2018. [4322](#)
- [37] Shaohui Liu, Xiao Zhang, Jianqiao Wangni, and Jianbo Shi. Normalized diversification. In *Proceedings of the IEEE Conference on Computer Vision and Pattern Recognition*, pages 10306–10315, 2019. [4322](#), [4323](#), [4324](#), [4325](#), [4327](#), [4328](#), [4332](#)
- [38] Ziwei Liu, Ping Luo, Xiaogang Wang, and Xiaoou Tang. Deep learning face attributes in the wild. In *Proceedings of International Conference on Computer Vision (ICCV)*, December 2015. [4327](#)
- [39] Dominik Lorenz, Leonard Bereska, Timo Milbich, and Björn Ommer. Unsupervised part-based disentangling of object shape and appearance. *arXiv preprint arXiv:1903.06946*, 2019. [4323](#)
- [40] Fujun Luan, Sylvain Paris, Eli Shechtman, and Kavita Bala. Deep photo style transfer. In *Proceedings of the IEEE Conference on Computer Vision and Pattern Recognition*, pages 4990–4998, 2017. [4322](#)
- [41] Fujun Luan, Sylvain Paris, Eli Shechtman, and Kavita Bala. Deep painterly harmonization. In *Computer Graphics Forum*, volume 37, pages 95–106. Wiley Online Library, 2018. [4322](#)
- [42] Qi Mao, Hsin-Ying Lee, Hung-Yu Tseng, Siwei Ma, and Ming-Hsuan Yang. Mode seeking generative adversarial networks for diverse image synthesis. In *Proceedings of the IEEE Conference on Computer Vision and Pattern Recognition*, pages 1429–1437, 2019. [4323](#), [4325](#), [4327](#), [4332](#), [4333](#)
- [43] Takeru Miyato, Toshiki Kataoka, Masanori Koyama, and Yuichi Yoshida. Spectral normalization for generative adversarial networks. *arXiv preprint arXiv:1802.05957*, 2018. [4325](#)
- [44] Kamyar Nazeri, Eric Ng, Tony Joseph, Faisal Qureshi, and Mehran Ebrahimi. Edgeconnect: Generative image inpainting with adversarial edge learning. *arXiv preprint arXiv:1901.00212*, 2019. [4322](#)
- [45] Deepak Pathak, Philipp Krahenbuhl, Jeff Donahue, Trevor Darrell, and Alexei A Efros. Context encoders: Feature learning by inpainting. In *Proceedings of the IEEE conference on computer vision and pattern recognition*, pages 2536–2544, 2016. [4322](#)
- [46] Guim Perarnau, Joost Van De Weijer, Bogdan Raducanu, and Jose M Álvarez. Invertible conditional gans for image editing. *arXiv preprint arXiv:1611.06355*, 2016. [4323](#)
- [47] Scott Reed, Zeynep Akata, Xinchun Yan, Lajanugen Logeswaran, Bernt Schiele, and Honglak Lee. Generative adversarial text to image synthesis. *arXiv preprint arXiv:1605.05396*, 2016. [4322](#)
- [48] Scott Reed, Zeynep Akata, Xinchun Yan, Lajanugen Logeswaran, Bernt Schiele, and Honglak Lee. Generative adversarial text to image synthesis. *arXiv preprint arXiv:1605.05396*, 2016. [4322](#)
- [49] Tamar Rott Shaham, Tali Dekel, and Tomer Michaeli. Singan: Learning a generative model from a single natural image. In *Proceedings of the IEEE International Conference on Computer Vision*, pages 4570–4580, 2019. [4324](#)
- [50] Eero P Simoncelli and William T Freeman. The steerable pyramid: A flexible architecture for multi-scale derivative computation. In *Proceedings., International Conference on Image Processing*, volume 3, pages 444–447. IEEE, 1995. [4321](#)
- [51] Yi-Hsuan Tsai, Xiaohui Shen, Zhe Lin, Kalyan Sunkavalli, Xin Lu, and Ming-Hsuan Yang. Deep image harmonization. In *Proceedings of the IEEE Conference on Computer Vision and Pattern Recognition*, pages 3789–3797, 2017. [4322](#)
- [52] Catherine Wah, Steve Branson, Peter Welinder, Pietro Perona, and Serge Belongie. The caltech-ucsd birds-200-2011 dataset. 2011. [4326](#)
- [53] C. Wah, S. Branson, P. Welinder, P. Perona, and S. Belongie. The caltech-ucsd birds-200-2011 dataset. Technical Report CNS-TR-2011-001, California Institute of Technology, 2011. [4333](#)
- [54] Jacob Walker, Carl Doersch, Abhinav Gupta, and Martial Hebert. An uncertain future: Forecasting from static images using variational autoencoders. In *European Conference on Computer Vision*, pages 835–851. Springer, 2016. [4323](#)
- [55] Xiaolong Wang, Rohit Girdhar, and Abhinav Gupta. Binge watching: Scaling affordance learning from sitcoms. In *Proceedings of the IEEE Conference on Computer Vision and Pattern Recognition*, pages 2596–2605, 2017. [4323](#)

- [56] Xiaolong Wang and Abhinav Gupta. Generative image modeling using style and structure adversarial networks. In *European Conference on Computer Vision*, pages 318–335. Springer, 2016. [4323](#)
- [57] Xintao Wang, Ke Yu, Shixiang Wu, Jinjin Gu, Yihao Liu, Chao Dong, Yu Qiao, and Chen Change Loy. Esrgan: Enhanced super-resolution generative adversarial networks. In *Proceedings of the European Conference on Computer Vision (ECCV)*, pages 0–0, 2018. [4322](#)
- [58] Huikai Wu, Shuai Zheng, Junge Zhang, and Kaiqi Huang. Gp-gan: Towards realistic high-resolution image blending. In *Proceedings of the 27th ACM International Conference on Multimedia*, pages 2487–2495, 2019. [4322](#)
- [59] Li Xu, Jimmy SJ Ren, Ce Liu, and Jiaya Jia. Deep convolutional neural network for image deconvolution. In *Advances in Neural Information Processing Systems*, pages 1790–1798, 2014. [4322](#)
- [60] Tianfan Xue, Jiajun Wu, Katherine Bouman, and Bill Freeman. Visual dynamics: Probabilistic future frame synthesis via cross convolutional networks. In *Advances in neural information processing systems*, pages 91–99, 2016. [4323](#)
- [61] Raymond A Yeh, Chen Chen, Teck Yian Lim, Alexander G Schwing, Mark Hasegawa-Johnson, and Minh N Do. Semantic image inpainting with deep generative models. In *Proceedings of the IEEE Conference on Computer Vision and Pattern Recognition*, pages 5485–5493, 2017. [4322](#)
- [62] Jiahui Yu, Zhe Lin, Jimei Yang, Xiaohui Shen, Xin Lu, and Thomas S Huang. Generative image inpainting with contextual attention. In *Proceedings of the IEEE Conference on Computer Vision and Pattern Recognition*, pages 5505–5514, 2018. [4322](#)
- [63] Xin Yu and Fatih Porikli. Ultra-resolving face images by discriminative generative networks. In *European Conference on Computer Vision*, pages 318–333. Springer, 2016. [4322](#)
- [64] Xin Yu and Fatih Porikli. Face hallucination with tiny unaligned images by transformative discriminative neural networks. In *AAAI*, volume 2, page 3, 2017. [4322](#)
- [65] Xin Yu and Fatih Porikli. Hallucinating very low-resolution unaligned and noisy face images by transformative discriminative autoencoders. In *Proceedings of the IEEE Conference on Computer Vision and Pattern Recognition*, pages 3760–3768, 2017. [4322](#)
- [66] Han Zhang, Tao Xu, Hongsheng Li, Shaoting Zhang, Xiaogang Wang, Xiaolei Huang, and Dimitris N Metaxas. Stackgan: Text to photo-realistic image synthesis with stacked generative adversarial networks. In *Proceedings of the IEEE International Conference on Computer Vision*, pages 5907–5915, 2017. [4322](#)
- [67] Han Zhang, Tao Xu, Hongsheng Li, Shaoting Zhang, Xiaogang Wang, Xiaolei Huang, and Dimitris N Metaxas. Stackgan++: Realistic image synthesis with stacked generative adversarial networks. *IEEE transactions on pattern analysis and machine intelligence*, 41(8):1947–1962, 2018. [4322](#), [4332](#), [4334](#)
- [68] Lingzhi Zhang, Jiancong Wang, and Jianbo Shi. Multimodal image outpainting with regularized normalized diversification. In *The IEEE Winter Conference on Applications of Computer Vision*, pages 3433–3442, 2020. [4322](#)
- [69] Lingzhi Zhang, Tarmily Wen, and Jianbo Shi. Deep image blending. In *The IEEE Winter Conference on Applications of Computer Vision*, pages 231–240, 2020. [4322](#)
- [70] Richard Zhang, Phillip Isola, Alexei A Efros, Eli Shechtman, and Oliver Wang. The unreasonable effectiveness of deep features as a perceptual metric. In *Proceedings of the IEEE Conference on Computer Vision and Pattern Recognition*, pages 586–595, 2018. [4326](#)
- [71] Jun-Yan Zhu, Richard Zhang, Deepak Pathak, Trevor Darrell, Alexei A Efros, Oliver Wang, and Eli Shechtman. Toward multimodal image-to-image translation. In *Advances in Neural Information Processing Systems*, pages 465–476, 2017. [4322](#), [4323](#), [4327](#)

Supplementary Materials: Nested Scale-Editing for Conditional Image Synthesis

In this section, we discuss the implementation details and demonstrate more qualitative results of our experiments on multimodal image outpainting, image super-resolution, cross-domain image translation, and text-to-image translation.

A. Image Outpainting

The detailed implementation of our decoder network architecture for image inpainting is shown in Fig.3 in the main paper. At each spatial scale, the number of channels for feature activation is 512. The conditional code is the feature vector of the occluded image encoded by a standard encoder network. The detailed implementations of the encoder network are listed in Table 4. We use negative slope of 0.2 for all LeakyReLU layers throughout the network. We employ the following abbreviation: N = Number of filters, K = Kernel size, S = Stride, P = Padding. "Conv" and "SN" denote convolutional layer and instance normalization respectively.

Layer	Hyper-parameters
1	Conv(N64-K4-S2-P1) + LeakyReLU
2	Conv(N128-K4-S2-P1) + IN + LeakyReLU
3	Conv(N256-K4-S2-P1) + IN + LeakyReLU
4	Conv(N512-K4-S2-P1) + IN + LeakyReLU
5	Conv(N256-K4-S2-P1) + IN + LeakyReLU
6	Conv(N256-K4-S2-P1) + IN + LeakyReLU
7	Conv(N128-K1-S2-P1) + LeakyReLU

Table 4: Encoder network for image outpainting and super-resolution.

The weights for the adversarial loss, disentangle loss, and diversity loss are all set to be ones. To enforce the diversity of synthesis, we sample $N = 4$ random variables at each iteration. We set the relaxation hyperparameter α in the diversity hinge loss to be 0.8. With batch size of 24, we train the network using Adam optimizer [29] with learning rate of $2e-4$, beta1 of 0.5, beta2 of 0.999.

B. Image Super-Resolution

Our super-resolution network is mostly similar to the network used for image outpainting with two major differences. The first difference is that we do not decode any image lower than the low-resolution scale (16x16), since there is no need to edit visual details below the input resolution scales. Thus, our decoder starts to generate images at scale of 32x32 and enforces the downsampled sample of the 32x32 images to be the same as the ground-truth 16x16 low-resolution image. The disentanglement loss for scales of 64 and 128 are the same as the outpainting network. In

addition, we add skip connections from the encoder to the decoder for the purpose of preserving low-resolution structural information. The encoder for the low-resolution image is the same as the encoder used in image outpainting, which is shown in Table 4. We also use the same optimizer and hyperparameters for both the image super-resolution and image outpainting.

C. Cross-Domain Translation

For the cross-domain translation task we adapted the MUNIT network [20]. In terms of network architecture, we use exactly the same content and style encoders as the original and we only modify the decoder, where we add an additional convolution for image output at the 128x128 resolution, and correspondingly the discriminator for it. We used the default multi-resolution discriminator as in the original implementation. For details of the architecture we refer reader to [20] and its official github repository¹. In terms of losses, in addition to the original reconstruction losses and discriminator losses, we calculated the proposed disentangle loss L_{disent} between the two levels as well as the normalized diversity loss [37] on each level. We use the following weights for losses: weight of adversarial loss $\lambda_{GAN} = 1$; weight of image reconstruction loss $\lambda_{xw} = 10$; weight of style reconstruction loss $\lambda_{sw} = 1$; weight of image reconstruction loss $\lambda_{cw} = 1$; weight of normalized diversity loss $\lambda_{ndiv} = 1$; weight of the disentangle loss $\lambda_{disent} = 1$. An illustration of the network architecture as well as the added losses is shown in Fig.9. We optimize the network using an Adam optimizer with learning rate of $1e-4$, beta1 of 0.5 and beta2 of 0.999 with batch size of 2.

D. Text-to-Image synthesis

Other than the image outpainting, image superresolution and cross-domain translation, we also evaluate our proposed multi-scale disentangle loss and the normalized diversity loss on the task of text-to-image synthesis. Our implementation is based on the StackGAN++ [67]. We refer interested reader to² for the original implementation. We use pretrain text embedding from [48], as in [67] and [42]. We keep the original text embedding sampling unchanged but incorporate two changes within the decoder. First, we incorporate the adaIn layer [19] for each refine stage, which allows injection of random latent vector at each stage. In comparison the original implementation only inject latent random vector at the init stage. Second, we added two more level of image output to the original image. The

¹<https://github.com/NVlabs/MUNIT>.

²<https://github.com/hanzhanggit/StackGAN-v2>

Method	Quality ↓	Diversity ↑
MSGAN [42]	18.64	0.661
Ours	20.88	0.668

Table 5: Quantitative comparison with state-of-the-art approaches on the cross-modal image-to-image translation task.

original StackGAN network outputs 64/128/256 images. We extended the network to output 16/32 images. With the two changes in place, we add the proposed disentangle loss and normalized diversification loss to it. Detailed architecture of the modified StackGAN++ is illustrated in Fig.10. We tested our network on the cub_200_2011 [53] birds dataset. As in the image outpainting, image super-resolution and cross-domain translation task, we achieve scale-specific editing by injecting different latent codes at each scale at test time, as shown on 14. Quantitatively, our network achieved similar image quality (measured by FID) and slightly higher diversity (measured by LPIPS) as previous state-of-the-art from [42], as shown by Table.5. We optimize the network using an Adam optimizer with learning rate of $2e - 4$, *beta1* of 0.5 and *beta2* of 0.999 with a batch size of 4.

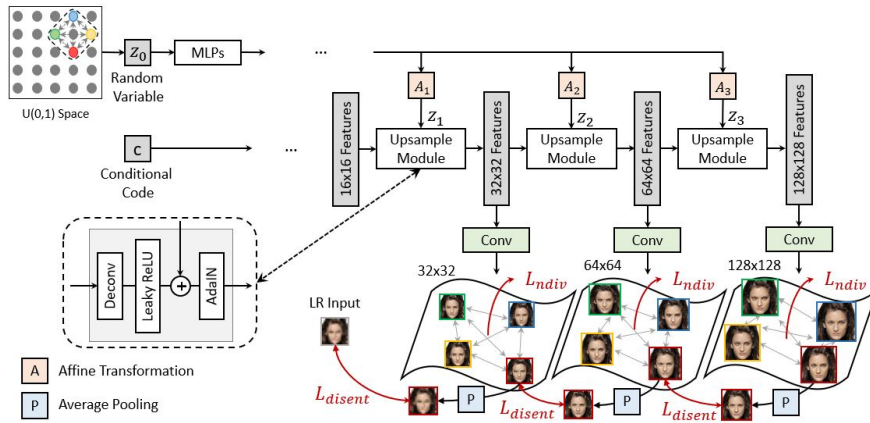


Figure 8: The model architecture of super-resolution decoder network.

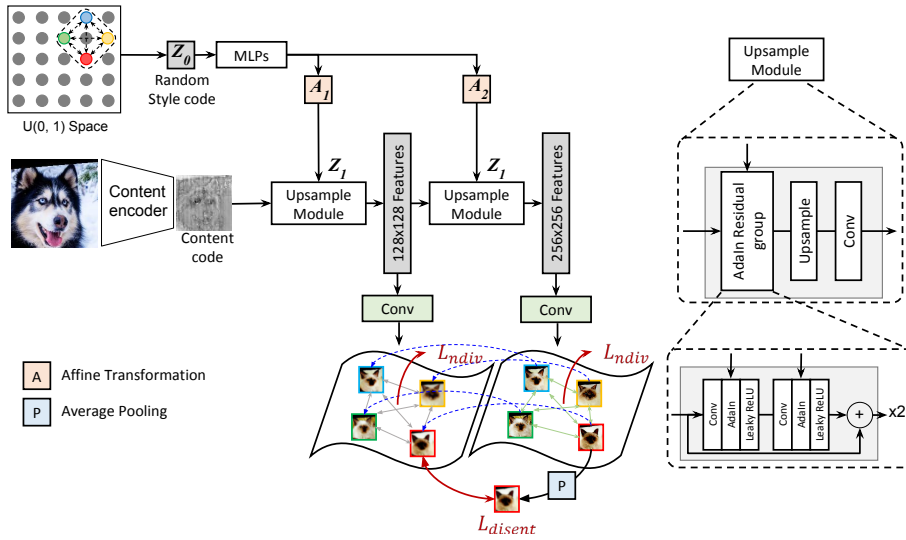


Figure 9: The model architecture of modified MUNIT [20] decoder network.

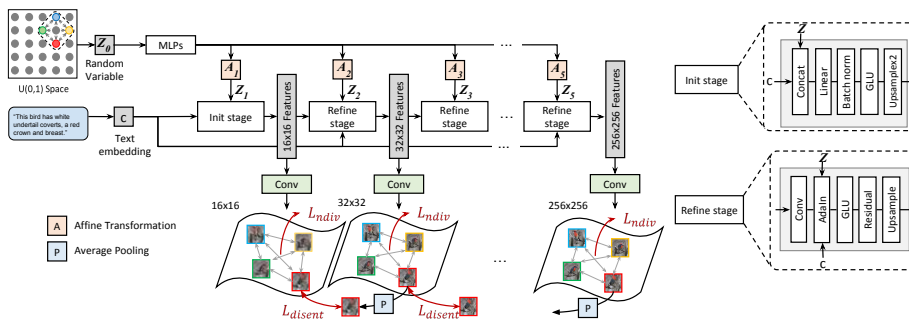


Figure 10: The model architecture of modified StackGAN++ [67] decoder network.

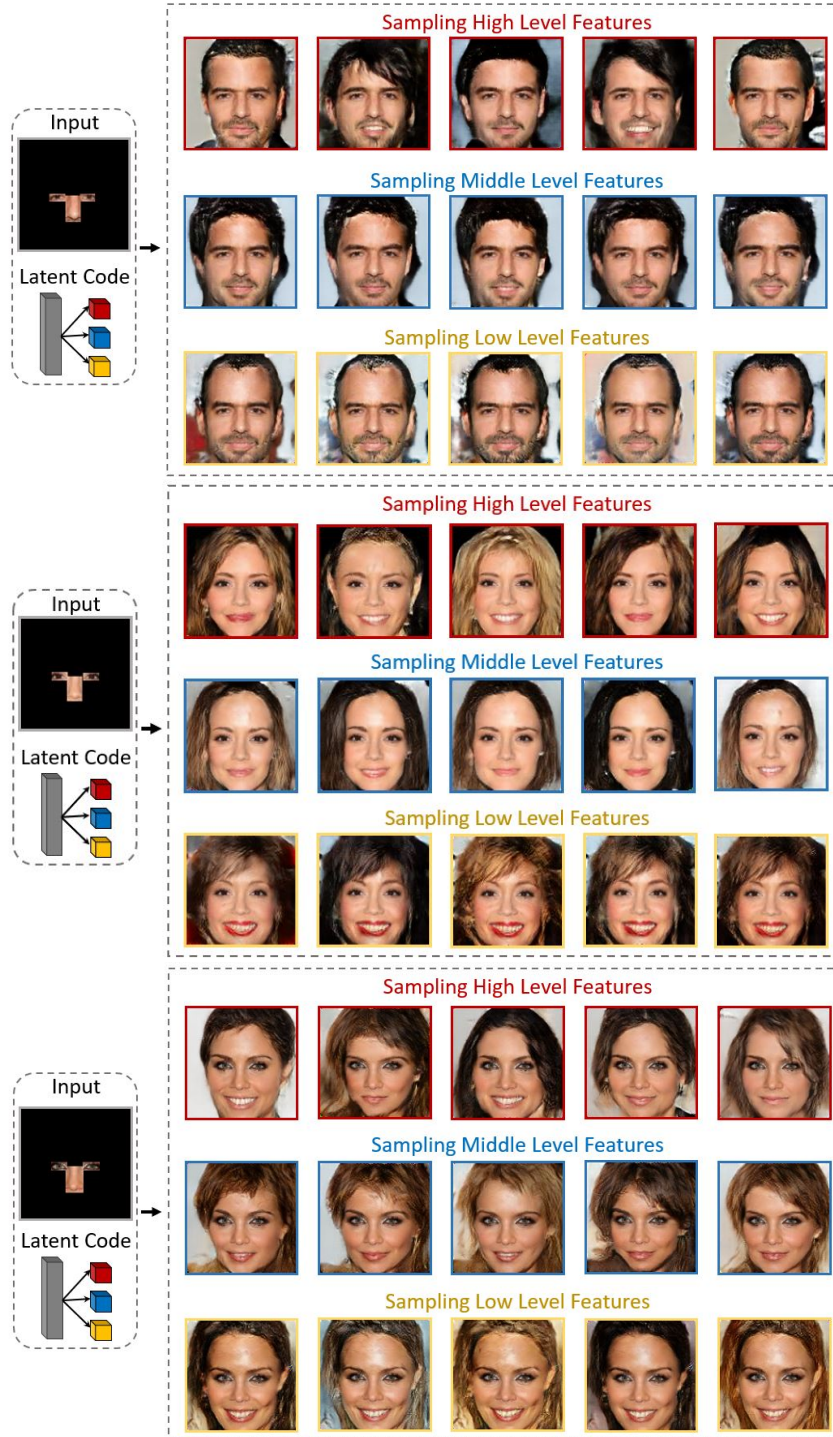


Figure 11: Qualitative results for scale-editing for image outpainting. We vary random variables at scale of 4 to edit high-level features, vary random variables at scale of 8 and 16 to edit the middle-level features, and vary random variables at scales of 32, 64, 128 to edit the low-level features.

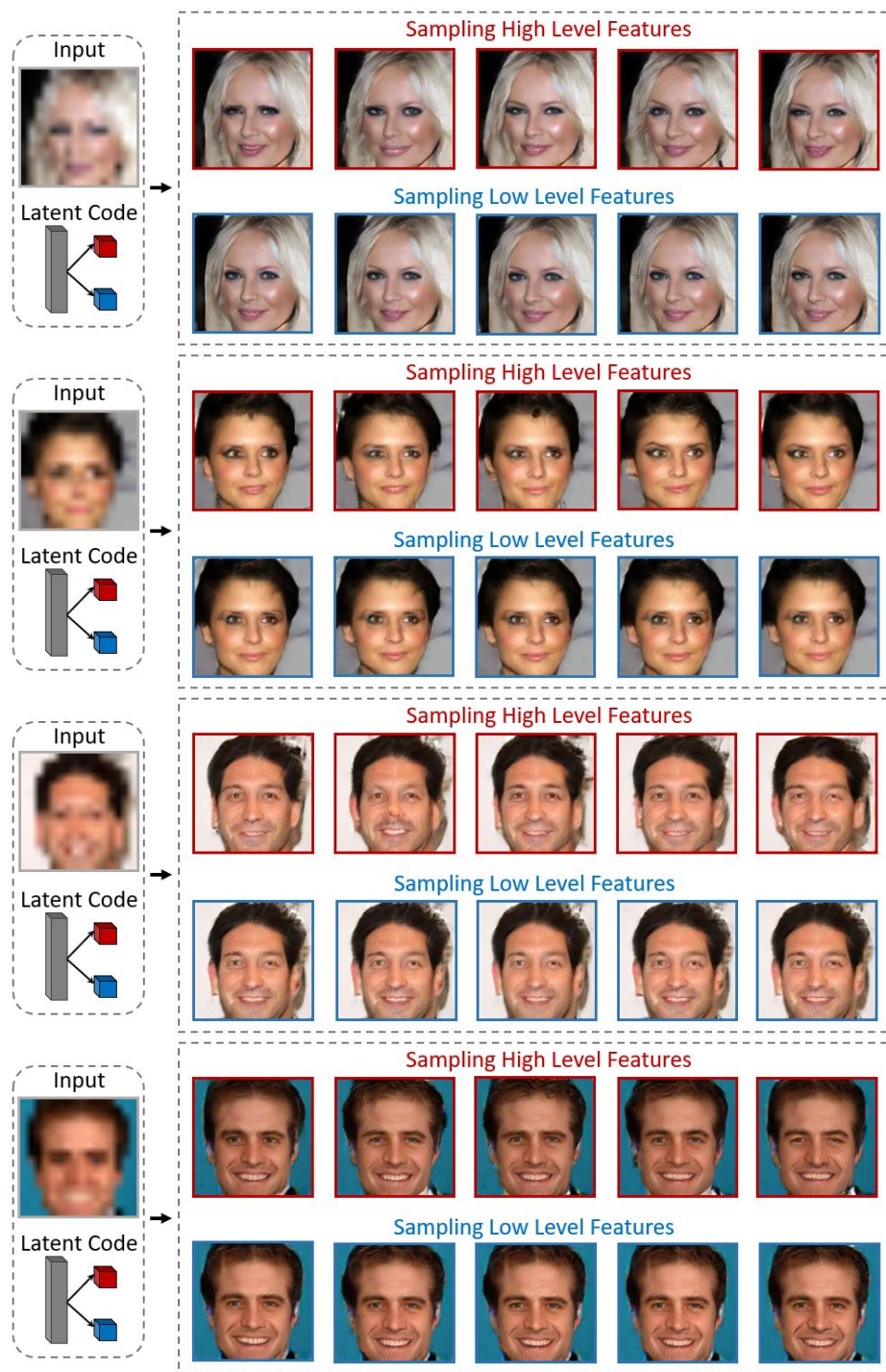


Figure 12: Qualitative results for scale-editing for image super-resolution. We vary random variables at scale of 32 to edit high-level features, and vary random variables at scales of 64 and 128 to edit the low-level features. Note that the variations for this task are small in nature, and the low-level features in this super-resolution task only affect subtle textures. In the super-resolution task, our main goal is to generate multimodal outputs while preserving identities.

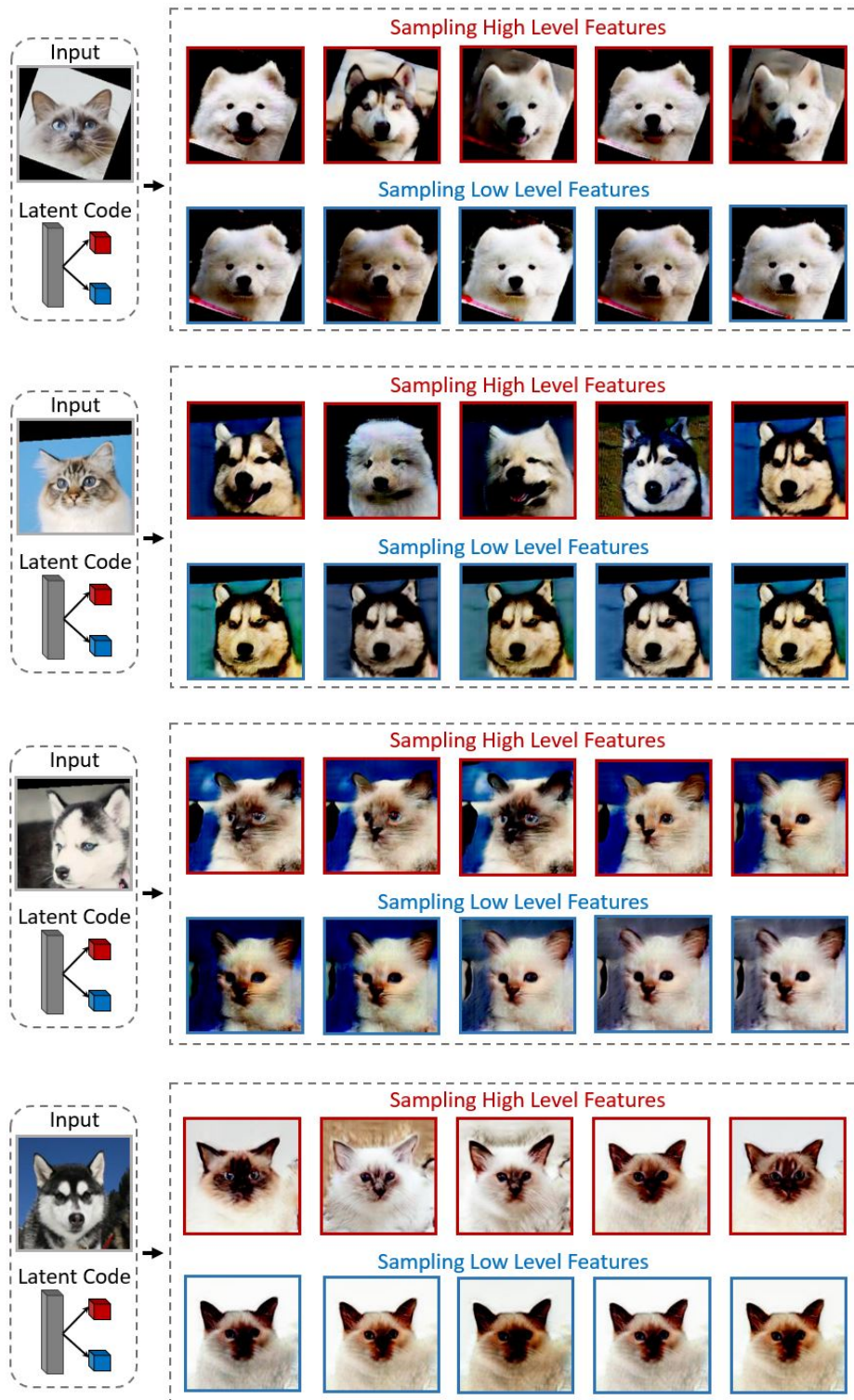


Figure 13: Qualitative results for scale-editing for cat2dog and dog2cat translation. Note that there are few modes of variation compared to other tasks, due to 1). primarily a small dataset size (871 cat and 1364 dog images) and 2). there are only two types of dogs (husky and samoyed) and mostly one type of cat (siamese) in the dataset.

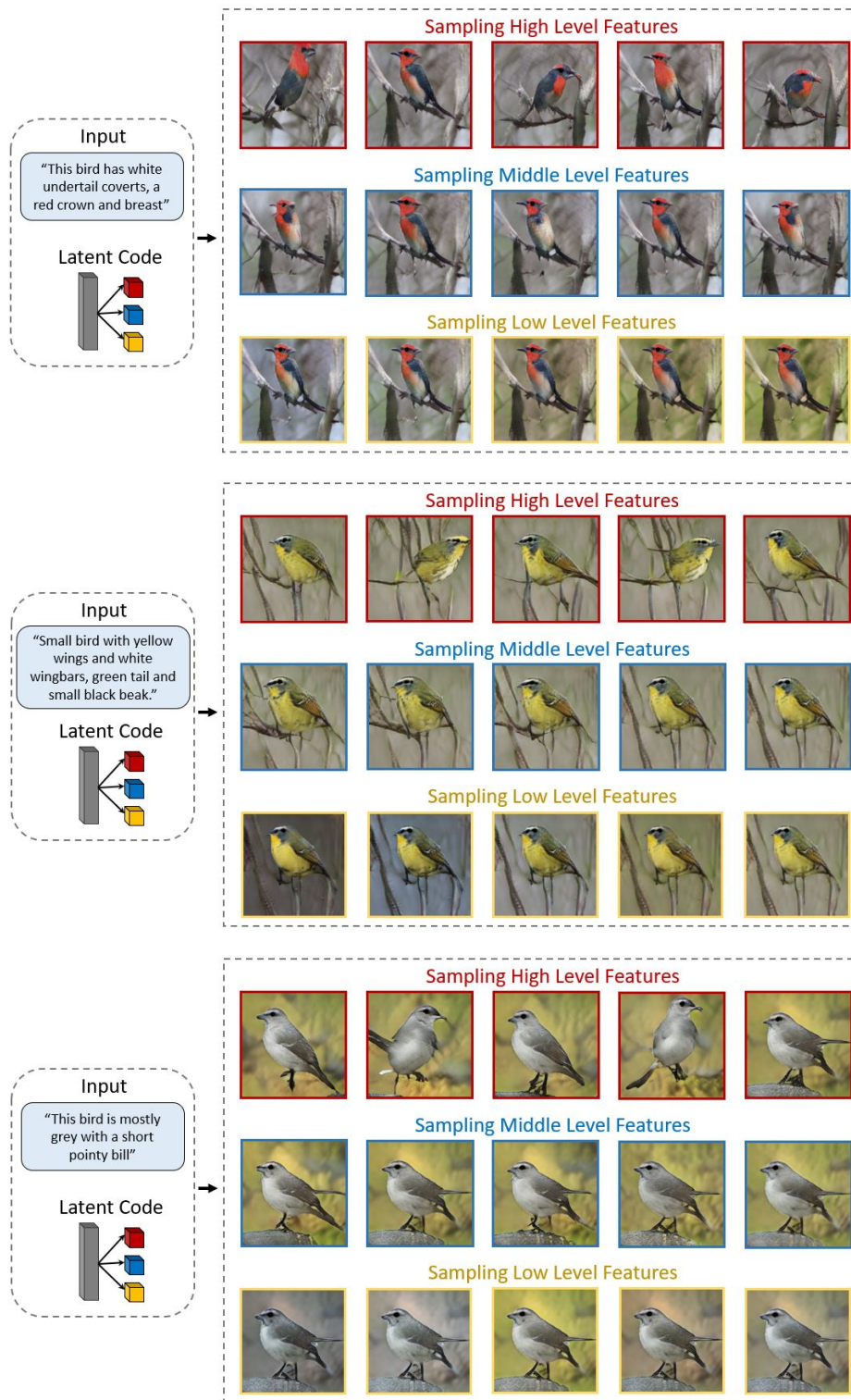


Figure 14: Qualitative results for scale-editing for text-to-image translation.